Human Molecular Genetics, 2018, Vol. 00, No. 00 1–20

doi: 10.1093/hmg/ddz111
Advance Access Publication Date: 25 May 2019
General Article

GENERAL ARTICLE

Phenotypic and biochemical analysis of an international cohort of individuals with variants in *NAA10* and *NAA15*

Hanyin Cheng[1,†], Leah Gottlieb[2,3,†], Elaine Marchi[4], Robert Kleyner[5], Puja Bhardwaj[5], Alan F. Rope[6,7], Sarah Rosenheck[5], Sébastien Moutton[8,9], Christophe Philippe[9,10], Wafaa Eyaid[11], Fowzan S. Alkuraya[12,13], Janet Toribio[14], Rafael Mena[15,16], Carlos E. Prada[17,18], Holly Stessman[19], Raphael Bernier[20], Marieke Wermuth[21], Birgit Kauffmann[21], Bettina Blaumeiser[22], R. Frank Kooy[23], Diana Baralle[24,25], Grazia M.S. Mancini[26], Simon J. Conway[27], Fan Xia[1,28], Zhao Chen[1,28], Linyan Meng[1,28], Ljubisa Mihajlovic[29], Ronen Marmorstein[2,3,30] and Gholson J. Lyon[4,5,*]

[1]Department of Molecular and Human Genetics, Baylor College of Medicine, Houston, TX 77030, USA, [2]Department of Chemistry, University of Pennsylvania, Philadelphia, PA 19104, USA, [3]Abramson Family Cancer Research Institute, Perelman School of Medicine, University of Pennsylvania, Philadelphia, PA 19104, USA, [4]Department of Human Genetics, New York State Institute for Basic Research in Developmental Disabilities, Staten Island, NY 10314, USA, [5]Stanley Institute for Cognitive Genomics, Cold Spring Harbor Laboratory, One Bungtown Road, Cold Spring Harbor, NY 11724, USA, [6]Kaiser Permanente Center for Health Research, Portland, OR 97227, USA, [7]Genome Medical, South San Francisco, CA 94080, USA, [8]Reference Center for Developmental Anomalies, Department of Medical Genetics, Dijon University Hospital, Dijon, France, [9]Génétique des Anomalies du développement, INSERM U1231, Lipides Nutrition et Cancer, UMR1231, Université de Bourgogne, F-21000, Dijon 21070, France, [10]Laboratoire de Génétique, Innovation Diagnostic Génomique des Maladies Rares UF6254, Plate-forme de Biologie Hospitalo-Universitaire, Centre Hospitalier Universitaire, Dijon 21070, France, [11]King Abdulaziz Medical City, King Saud Bin AbdulAziz University—Health Science, King Abdullah International Medical Research Center, Riyadh 11426, Saudi Arabia, [12]Department of Genetics, King Faisal Specialist Hospital and Research Center, Riyadh 11211, Saudi Arabia, [13]Department of Anatomy and Cell Biology, College of Medicine, Alfaisal University, Riyadh 11533, Saudi Arabia, [14]Division of Cardiology, CEDIMAT, Santo Domingo 51000, Dominican Republic, [15]Neonatal Intensive Care Unit, Centro de Obstetricia y Ginecologia, Santo Domingo, Dominican Republic, [16]Division Of Neonatology, Cincinnati Children's Hospital Medical Center, Cincinnati, OH 45229, USA, [17]Division of Human Genetics, Cincinnati Children's Hospital Medical Center, Cincinnati, OH 45229, USA, [18]Department of Pediatrics, University of Cincinnati College of Medicine, Cincinnati, OH 45229, USA, [19]Department of Pharmacology, Creighton University Medical School, Omaha, NE 68178, USA, [20]Department of Psychiatry, University of Washington, Seattle, WA 98195, USA,

[†]These authors contributed equally.
Received: February 4, 2019. **Revised:** April 29, 2019. **Accepted:** May 20, 2019

[21]Klinik für Kinder-und Jugendmedizin, Neuropädiatrie, Klinikum Links der Weser, Senator-Weβling-Str.1. in 28211 Bremen, Germany, [22]University and University Hospital of Antwerp, Antwerp, Belgium, [23]Department of Medical Genetics, University of Antwerp, Antwerp 2000, Belgium, [24]Human Development and Health, Faculty of Medicine, University of Southampton, Southampton SO16 5YA, UK, [25]Wessex Clinical Genetics Service, Princess Anne Hospital, Southampton, UK, [26]Department of Clinical Genetics, Erasmus MC University Medical Center, Rotterdam 3015 GD, The Netherlands, [27]HB Wells Center for Pediatric Research, Indiana University School of Medicine, Indianapolis, IN 46202, USA, [28]Baylor Genetics, Houston, TX 77021, USA, [29]GeneInfo, Human Genetics, 18000 Niš, Serbia and [30]Department of Biochemistry and Biophysics, Perelman School of Medicine, University of Pennsylvania, Philadelphia, PA 19104, USA

*To whom correspondence should be addressed at: Department of Human Genetics, New York State Institute for Basic Research in Developmental Disabilities, Staten Island, NY 10314, USA. Tel: +1 7184945388; Fax: +1 7184941026; Email: gholsonjlyon@gmail.com

Abstract

N-alpha-acetylation is one of the most common co-translational protein modifications in humans and is essential for normal cell function. *NAA10* encodes for the enzyme NAA10, which is the catalytic subunit in the N-terminal acetyltransferase A (NatA) complex. The auxiliary and regulatory subunits of the NatA complex are NAA15 and Huntington-interacting protein (HYPK), respectively. Through a genotype-first approach with exome sequencing, we identified and phenotypically characterized 30 individuals from 30 unrelated families with 17 different *de novo* or inherited, dominantly acting missense variants in *NAA10* or *NAA15*. Clinical features of affected individuals include variable levels of intellectual disability, delayed speech and motor milestones and autism spectrum disorder. Additionally, some subjects present with mild craniofacial dysmorphology, congenital cardiac anomalies and seizures. One of the individuals is an 11-year-old boy with a frameshift variant in exon 7 of *NAA10*, who presents most notably with microphthalmia, which confirms a prior finding with a single family with Lenz microphthalmia syndrome. Biochemical analyses of variants as part of the human NatA complex, as well as enzymatic analyses with and without the HYPK regulatory subunit, help to explain some of the phenotypic differences seen among the different variants.

Introduction

N-alpha-acetylation is a common co-translational protein modification that is essential for normal cell function in humans. *NAA10* encodes for the enzyme NAA10, which acts as the catalytic subunit of N-terminal acetyltransferase A (NatA) for the co-translational N-acetylation of proteins with Ser, Ala, Thr, Gly and Val N-termini, in addition to other functions (1,2). *NAA10*-related syndrome (3) is an X-linked condition with a broad spectrum of findings ranging from a severe phenotype in males with p.Ser37Pro in NAA10, originally described as Ogden syndrome (4), to the milder *NAA10*-related intellectual disability (ID) found with different variants in both males and females (5–12). There is also one previously reported family with Lenz microphthalmia syndrome (LMS) with a mutation in the intron 7 splice donor site (c.471+2T>A) of *NAA10* (13). Although postnatal developmental impairments and ID may be the presenting feature (and in some cases the only finding), many individuals exhibit additional differences including *in utero* instigated cardiovascular, growth and dysmorphic findings, each of which vary in type and severity; therefore, this set of disorders has substantial phenotypic variability and as such should be referred to more broadly as *NAA10*-related syndrome (3). The auxiliary subunit of the NatA complex, NAA15, is responsible for the induction of conformational changes into NAA10, including active site rearrangement for canonical NatA complex substrate-binding specificity (14). The Huntington-interacting protein (HYPK) regulatory subunit inhibits intrinsic NatA activity and is proposed to modulate cognate NatA activity (15). We recently identified and phenotypically characterized 38 individuals from 33 unrelated families with 25 different *de novo* or inherited, dominantly acting likely gene disrupting (LGD) variants in *NAA15* (16). Clinical features of affected individuals with LGD variants in *NAA15* included variable levels of ID, delayed speech and motor milestones and autism spectrum disorder (ASD). Additionally, mild craniofacial dysmorphology, congenital cardiac anomalies and seizures are present in some subjects. In the present study, we have collected phenotypic information on individuals with missense variants in *NAA10* and *NAA15*, and we report herein 23 new individuals with *NAA10*-related syndrome, while also reporting 7 different missense variants in *NAA15* that are likely associated with various neurodevelopmental phenotypes. To complement these findings and provide a survey of both the previously and newly reported variants, we have also conducted biochemical analyses of some of these variants, as part of the human NatA complex, as well as enzymatic studies with and without the HYPK regulatory protein (15,17,18). These functional results help to explain some of the wide-ranging phenotypic differences observed among the different variants.

Results

NAA10 and NAA15 variants

We ascertained 22 individuals from 22 unrelated families with 9 different missense variants in *NAA10*, along with 1 other

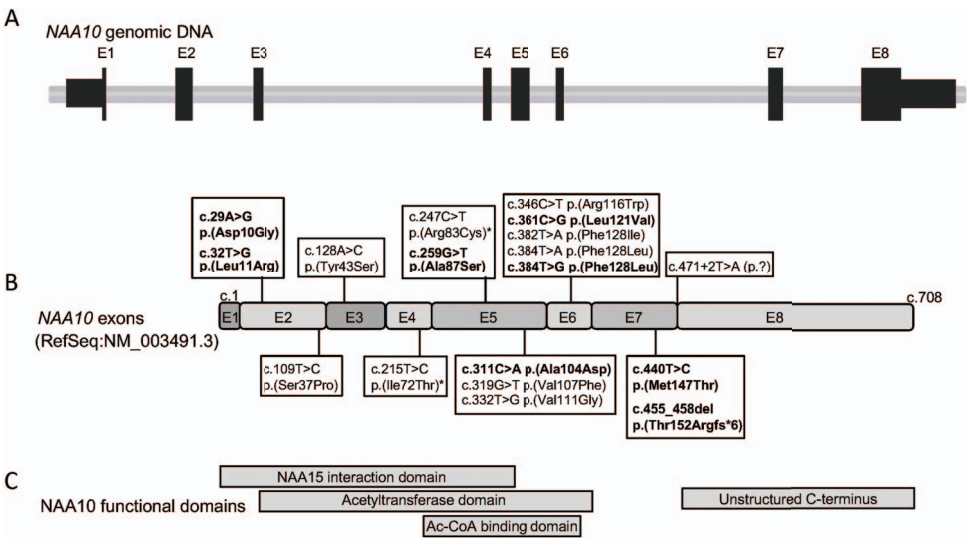

Figure 1. *NAA10* mutations identified in this study. (**A**) Schematic representation of the genomic structure of human *NAA10*. Solid rectangles indicate exons, and the horizontal bars represent introns. (**B**) Exonic localization of *NAA10* mutations identified in this study and those previously reported elsewhere. Novel mutations identified in this study are marked in bold. * indicated published mutations in which new information is provided in this study. (**C**) The functional domains of human NAA10 protein.

family with 1 male with a frameshift variant in *NAA10*. From these 23 families with variants in *NAA10*, 19 of these were *de novo*, 2 were maternally inherited and the remaining 2 had an unknown inheritance. None of the variants in *NAA10* were reported in public control databases such as Genome Aggregation Database (gnomAD). Figure 1 shows the location of these variants in *NAA10*. Seven individuals from seven unrelated families with missense variants in *NAA15* were ascertained. In the seven individuals with *NAA15* variants, four of these were *de novo*, one was maternally inherited, one was paternally inherited and one had an unknown inheritance pattern. For *NAA15*, five of the variants were not present in public control databases such as gnomAD, whereas the c.1348A>G p.(Lys450Glu) and c.1424C>T p.(Ala475Val) variants were present only once and twice, respectively, in gnomAD. Phenotypic information as well as the variant inheritance is not available on these individuals in ExAC or gnomAD. Information regarding these *NAA10* or *NAA15* variants is given in Table 1 and Supplementary Material, Table S1.

Clinical features

Although each variant will be discussed below and in the Supplementary Material in greater detail, most individuals with variants involving *NAA10* or *NAA15* have variable degrees of neurodevelopmental disabilities, including impaired motor abilities (HP:0001270), ID (HP:0001249), impaired verbal abilities (HP:0000750) and ASD (HP:0000729) (Table 1; Supplementary Material, Table S1). The males with variants in *NAA10* are predictably much more severely affected, due to having only one X-chromosome, and some of these individuals died in infancy. Many subjects have impaired motor function, including fine motor difficulties, abnormality of movement, motor delay and hypotonia. Various levels of ID are reported in almost all study subjects with available data, including mild, moderate or severe ID, and learning difficulties with or without behavioral issues (Tables 1 and 2; Supplementary Material, Table S1). Most affected individuals have verbal issues including complete absence of speech, delayed language development, required use of sign language or other speech difficulties. The common and less common features in the cohort are summarized in Table 2. Most subjects also present with either ASD and/or other behavioral challenges. A recognizable, regular pattern of dysmorphic facial features was not appreciated among the cases. That being said, commonly seen traits include thicker eyebrows and broad philtra (Fig. 2). The birth weight was low (≤5th percentile) in a few individuals, and it was noted that some individuals failed to grow, so that their weights fell below the 5th percentile over time (Supplementary Material, Table S1).

Clinical presentation of individuals with variants in *NAA10*

One family presented with a boy (Individual 1) with a c.29A>G p.(Asp10Gly) variant who died in the first 6 months of life (Fig. 2). This boy had agenesis and hypoplasia of the corpus callosum, ventriculomegaly, delayed motor development, muscular hypotonia, ptosis, hearing loss, hypertension, right-sided ventricular hypertrophy due to primary pulmonary hypertension, with eventual right-sided heart failure and death, and dysmorphic features (broad nose, broad forehead and long philtrum). This boy's facial features were remarkably similar to the boys with Ogden syndrome, which was originally named for two families with boys with the c.109T>C p.(Ser37Pro) variant (4,19).

A 3-year-old girl (Individual 2) was discovered to have a c.32T>G p.(Leu11Arg) variant (see Fig. 2). Hydrocephalus developed in part due to a large arachnoid cyst between the cerebellum and the occipital area, leading to increased intracranial pressure and requiring ventriculo-peritoneal drainage at the age of 2 months. Ventriculomegaly was already present at ultrasound in the 35th gestational week (GW); she was born in the 39th GW with a normal head circumference (HC) of 33 cm. After drainage, the brain Magnetic Resonance Imaging (MRI) scan showed hypoplasia of the corpus callosum, hyperplasia of the choroid plexus and partial agenesis of the septum pellucidum. At the ages 2.7 and 3 years, respectively, her HC measured at −1.4 Standard Deviation (SD) and her height at −1.8 SD. She

Table 1. Summary of clinical features and molecular findings in individuals with NAA10 variants in this study

ID	Age/sex	Variant and inheritance	Feeding	MRI	Neurodevelopmental	Cardiac	Eye	Others
1	4 months/M	c.29A>G p.(Asp10Gly), *de novo*	Difficulty swallowing, at risk for aspiration	MRI: agenesis of corpus callosum, hypoplastic corpus callosum, ventriculomegaly	Hypotonia	ECG: right ventricular hypertrophy due to primary pulmonary hypertension, with eventual right-sided heart failure and death	N/A	Dysmorphic facial features, barrel chest, bilateral profound sensorineural hearing loss
2	3 years/F	c.32T>G p.(Leu11Arg), Unknown inheritance	No difficulties	MRI: congenital hydrocephalus, ventriculomegaly, hypoplasia of the corpus callosum, hyperplasia of the choroid plexus and partial agenesis of the septum pellucidum	Delayed motor development, walked at around age 3 years, speech delay	N/A	Strabismus	N/A
3	4.2 years/M	c.215T>C p.(Ile72Thr), Maternal inheritance	Gastrostomy tube care	MRI: medulloblastoma	ID, ataxia, mild motor delay, marked speech delay	ECG: enlarged heart muscle, tachycardia, prolonged QT interval, died due to cardiopulmonary issues	Strabismus,	Dysmorphic facial features, posterior fossa syndrome, loss of height between T5 and T6
4	10 years/F	c.247C>T p.(Arg83Cys), *de novo*	Functional bulbar palsy, esophagus and gut dysmotility syndrome, complete dysphagia	MRI: normal	Global developmental delay, severe intellectual disabilities, poor fine motor skills, apraxia	None	Cortical/cerebral visual impairment, bilateral astigmatism, alternating divergent squint	Behavioral issues (autistic traits, severe sensor processing issues, anxiety), severe sleep disorder, short statue, bilateral talipes, reflux and constipation issues, kyphosis, hypertrichosis, mixed muscle tone
5	13 years/F	c.247C>T p.(Arg83Cys), *de novo*	percutaneous endoscopic gastrostomy (PEG) feeding	MRI: generalized lack of white matter bulk with thinning of the corpus callosum and prominent Cerebrospinal fluid (CSF) spaces	Severe global development delay, severe motor delay, poor fine motor skills, very limited speech	ECG: prolonged QT interval, bicuspid valve	Moderate astigmatism, borderline electro-diagnostics	Absence seizures, pectus excavatum, premature precocious puberty, remains incontinent

Continued.

Continued.

ID	Age/sex	Variant and inheritance	Feeding	MRI	Neurodevelopmental	Cardiac	Eye	Others
6	11.5 years/F	c.247C>T p.(Arg83Cys), *de novo*	PEG feedings, gastrointestinal dysmotility (GI) dysmotility, cyclical vomiting, food intolerance, allergic to most antibiotics	MRI: small cyst	Global developmental delay, poor fine motor skills, ID, non-verbal, but can read and type in full sentence	N/A	Cortical visual impairment	Micrognathia, moderate to severe hearing impairment; precocious puberty, body odor, autistic traits
7	34 years/F	c.247C>T p.(Arg83Cys), *de novo*	Excessive vomiting, gastro-esophageal reflux, coeliac disease	N/A	Global developmental delay, motor delay, severe mental retardation, no understandable speech	ECG: normal	N/A	Facial dysmorphism, epilepsy, increased muscle tone and contracture, sleep disturbance
8	13 years/F	c.247C>T p.(Arg83Cys), *de novo*	Gut dysmotility, food intolerance, frequent vomiting, severe allergies	N/A (not performed)	Global developmental delay, motor delay, learning disability, limited speech	ECG: long QT syndrome	Astigmatism, hyperopia	Toe walking, high anxiety, stereotypical behaviors, leg discrepancy, frequent nose bleeds, pica, noise sensitivity, cutis marmorata
9	15 years/F	c.247C>T p.(Arg83Cys), *de novo*	N/A	N/A	Global developmental delay, unable to manage tasks independently such as dressing, toileting and feeding, non-verbal	Tetralogy of Fallot surgically corrected at age 4 months	N/A	ASD, challenging behaviors including pulling hair and a trichobezoar—laparotomy required; no sense of danger
10	7.5 years/F	c.247C>T p.(Arg83Cys), *de novo*	Feeding difficulties	Ventriculomegaly and intracranial hemorrhage at birth; ventriculoperitoneal (VP) shunt inserted at age 1 month	Severe global development delay, significant motor delay, hypotonia, cannot sit up alone, severe cognitive impairment, non-verbal	None	Central vision impairment, astigmatism and farsighted	Partial epilepsy, growth delay microcephaly, hydrocephalus status post shunt surgery
11	1.2 years/F	c.247C>T p.(Arg83Cys), *de novo*	Feeding difficulties, fed with thick juices or puree	MRI: normal	Global development delay, motor delay	ECG: secundum ASD with left to right shunt, mild valvular pulmonary stenosis, dilated right atrium and ventricle, good left ventricular (LV)/right ventricular (RV) function	N/A	Facial dysmorphism, bilateral minimal hearing loss
12	6 years/F	c.247C>T p.(Arg83Cys), *de novo*	Failure to thrive, manages finger soft baby food	N/A	Global developmental delay, motor delay, attending special education class, non-verbal	ECG: long QT syndrome	N/A	Facial dysmorphism, seizures, extra rib, extra vertebrae, possible anterior beaking L1 vertebrae, behavioral issues

Continued.

Continued.

ID	Age/sex	Variant and inheritance	Feeding	MRI	Neurodevelopmental	Cardiac	Eye	Others
13	2.5 years/F	c.247C>T p.(Arg83Cys), *de novo*	Feeding difficulties, gastric reflux disease, esophagitis	N/A	Global developmental delay, mild hypotonia, speech delay, partially non-verbal ID		Astigmatism	Growth delay, sensory processing disorder, avoidance disorder, facial dysmorphism
14	7 years/F	c.247 C>T p.(Arg83Cys), *de novo*	Feeding difficulties; food allergies, soy	MRI: subtle abnormalities in white matter of both the occipital and temporal lobes; there was a decrease in the central white mass volume and a thinning of the corpus callosum	Microcephaly, developmental delay, mild hypotonia, mild cerebral palsy, non-verbal ASD ID		Astigmatism, myopia corrected with eyeglasses	Growth delay; sensory processing disorder; avoidance disorder; sensory seeking behaviors; microcephaly, facial dysmorphism
15	15 years/F	c.259G>T p.(Ala87Ser), *de novo*	Feeding difficulty in infancy, abnormality of the gastrointestinal tract	MRI: normal	Severe global developmental delay, gross motor development delay, severe ID, non-verbal, generalized hypotonia, spastic paraplegia	ECG: normal cardiovascular examination: normal	Optic nerve hypoplasia	Facial dysmorphism; epilepsy, tonic clonic seizures; bilateral sensorineural hearing impairment; ADHD, autistic behavior, unpredictable behavior under stress
16	2.5 years/F	c.259G>T p.(Ala87Ser), *de novo*	No trouble swallowing, some feeding issues due to coordination	MRI: hypoplasia of corpus callosum, and mild myelination defect	Global developmental delay, hypotonia, non-verbal	N/A	None	Mildly dysmorphic; relatively short stature, significantly elevated alkaline phosphatase
17	14 years/F	c.259G>T p.(Ala87Ser), *de novo*	Swallowing difficulties eats mashed food only	MRI: subcortical hyper intensities in the white matter and basal ganglia; periventricular and pallidum (cysts)	Global developmental delay, severe cognitive disability, dystonic movement disorder, non-verbal	ECG: normal	None	Growth delay, myoclonic epilepsy, degenerative course due to three dystonic crisis, life-threatening dystonic status, severe scoliosis, mixed muscle tone, wheelchair bound
18	10 years/F	c.311C>A p(.Ala104Asp), *de novo*	Chewing and swallowing difficulties	MRI: normal	Global developmental delay, hypotonia, fine motor delay, ID, mixed receptive and expressive language disorder, apraxia	ECG: normal	Astigmatism anisometropia conjunctivae and EOM noted as normal on examination	ADHD (combined type), stereotypies, anxiety, Sensory processing disorder, growth hormone deficiency, relatively short stature, hip dysplasia, hearing impairment, sleep disorder

Continued.

Continued.

ID	Age/sex	Variant and inheritance	Feeding	MRI	Neurodevelopmental	Cardiac	Eye	Others
19	6 years/F	c.361C>G p.(Leu121Val), *de novo*	Gut issues, which have been better with supplements, silent reflux as an infant	MRI: normal	Global developmental delay, severe ID, motor delay and poor coordination, non-verbal	ECG: normal	N/A	Facial dysmorphism, toe walking, severe autism, self-stimulatory behavior, mixed muscle tone, hip dysplasia, severe sleep issues
20	14 years/F	c.361C>G p.(Leu 121 Val), Unknown inheritance	No feeding issues		Delayed motor development, mild hypotonia, speech delay partially non-verbal ID, ASD, avoidance disorder		Optokinetic nystagmus	Growth delay, sensory processing disorder, anxiety, avoidance disorder
21	1.3 years/F	c.384T>G p.(Phe128Leu), *de novo*	Nasogastric tube feedings as infant, gastric reflux	MRI: bilateral pyramidal characteristics with deviations in the basal ganglia	Delayed motor development	ECG: normal QT interval: normal cardiac exam	Cortical vision impairment	Microcephaly, relatively short stature, poor eye contact, chorea; overriding toes; single crease hand line
22	8 years/F	c.440T>C p.(Met147Thr), *de novo*	Unable to drink from a bottle due to coordination issue, learned to chew through Applied Behavioral Analysis (ABA) therapy	MRI: thinning of corpus callosum	Overall developmental delay, moderate intellectual impairment with advanced math skills, coordination issues, limited speech	ECG: normal	stigmatism, cortical visual impairment	Sensory processing disorder, self-stimulating behaviors, but very social and no other evidence of autism, microcephaly, acne, body odor, adrenarche, light sleeper
23	11 years/M	c.455_458del p.(Thr152Argfs*6), Maternal inheritance	Low appetite, no chewing or swallowing issues	MRI: agenesis of corpus callosum, craniosynostosis	Global developmental delay, severe ID, generalized hypotonia, wheelchair bound	ECG: defect in the atrial septum	Microcornea, microphthalmia	Growth delay

Table 2. Summary of the relative prevalence of each phenotype in 23 individuals with *NAA10* variants

Phenotype	Number of individuals with phenotype	Number of individuals with relevant data	Percentage
Brain structure and function			
Global developmental delay	23	23	100%
Non-verbal or limited speech	21	21	100%
ASD, ADHD and other behavioral issues	22	22	100%
Abnormal MRI	14	18	77%
Seizures	9	13	69%
Motor impairments			
Feeding difficulties	23	23	100%
Motor delay and related abnormalities	23	23	100%
Muscle tone issues	17	17	100%
Cardiovascular			
Long QT syndrome	7	19	37%
Heart failure and death	2	23	4%
Atrial septum defect	3	18	17%
Pulmonary hypertension	1	17	6%
Tetralogy of Fallot	1	17	6%
Other			
Facial dysmorphism	23	18	78.20%
Eye abnormalities	15	17	88.20%
Skeletal or connective tissues disorders	9	15	60%
Growth delay[a]	13	23	56.50%
Sleep disorder	7	16	43.70%
Hearing impairment	8	19	42.10%

[a]Growth delay is indicated in individuals whose height and weight is below 3 percentile at last visit.

presented a mild pyramidal syndrome but walked at around 3 years of age, has strabismus and has no speech development at the age of 4 years. She experienced feedings difficulties. Renal ultrasound and cardiology screening, including ECG and echocardiography, were normal.

One of the males (Individual 3) was determined to have a c.215T>C p.(Ile72Thr) variant, and this male was previously reported (as Patient II-1) (11). His picture is shown in Figure 2. He had some coarse facial features with an abnormally shaped head with a small chin, high arch palate and prominent musculature. More information can be found in Supplementary Material. Most notably, he had a history of cardiomyopathy, tachycardia and a prolonged QT interval (493 ms was last reported QT interval, and it was never above 500 ms). He died suddenly at the age of 3 years in January 2018 due to cardiopulmonary issues, likely due to complications from the cardiomyopathy. It is uncertain however if there was an arrhythmia event that preceded this decompensation. An autopsy was not performed. The mother, who is a carrier of the variant, reported that she graduated college and was gainfully employed for 12 years thereafter. She had test-related anxiety during schooling and did receive math tutoring, but there is no evidence for ID or any learning disability and there was never any formal IQ testing.

We obtained clinical information on 10 females (Individuals 4–14) with the c.247C>T p.(Arg83Cys) variant, which was *de novo* in all of them. Facial photographs are presented in Figure 2 for those with consent to publish photographs. The clinical presentation of these girls is similar to what has been presented with other children with this variant (5).

We identified three individuals with *de novo* c.259G>T p.(Ala87Ser) variants. The first is a 14-year-old girl (Individual 15) (see Fig. 2). She was born after an unremarkable pregnancy and a normal delivery. She is diagnosed with global developmental delay, epilepsy with tonic clonic seizures, attention deficit hyperactivity disorder (ADHD), ASD, fine motor delay, bilateral hearing impairment, absent speech and optic nerve hypoplasia. In terms of facial dysmorphology, she has a thin vermillion, microcephaly, malar flattening and long philtrum. She has normal cardiac function and a normal corrected QT interval (QTC). Despite being on medication, the seizures still occur daily.

The second individual is a 2.5-year-old female (Individual 16) also with a *de novo* heterozygous c.259G>T p.(Ala87Ser) variant. She is diagnosed with global developmental delay, hypotonia, relative microcephaly, mild dysmorphic features and has significantly elevated alkaline phosphatase levels. She is essentially non-verbal but can say 'da-da'. At age 1, she could not crawl or sit up independently. At age 2, she could crawl, pull to stand and cruise along furniture, but she is not able to stand or walk independently. A brain MRI showed hypoplasia of corpus callosum and a mild myelination defect. The child has a happy disposition and readily smiles. She receives physical therapy and speech therapy.

The third recurrent variant is in a 14-year-old female (Individual 17) with a *de novo* heterozygous c.259G>T p.(Ala87Ser) variant. She has severe global developmental disorder. Her first symptoms occurred in the 5th week of life with muscle hypotonia and difficulty swallowing. At age 4 years, free walking with a dystonic broad-based gait was reported. She was also diagnosed with urinary and fecal incontinence, has no expressive speech and has severe scoliosis. She had a dystonic movement disorder with a degenerative course due to three dystonic crisis at the age of 8.5 years, 10 years and 12 years, respectively, which worsened with each crisis: at the age of 12 years she developed a myoclonus epilepsy with generalized sharp waves noted on the Electroencephalogram (EEG), which was treated with valproic acid and topiramate. Her general condition worsened; her behavior included biting, hair pulling and

Figure 2. Facial morphology of individuals with *de novo* or inherited *NAA10* missense variants. A recognizable, regular pattern of dysmorphologic facial features was not discerned among the cases, other than perhaps thicker eyebrows and broad philtra. Individual 1: top picture at age 1 month, bottom picture at age 3.3 months. The child died at age 4 months due to heart failure. Individual 3: top picture at age 3 years old. Bottom picture at age 3 years, 11 months. This child died a few months later due to cardiopulmonary issues. Individual 4: at age 7 years old. Individual 5: top picture, age 10; bottom picture, age 12. Individual 6: at age 11 in both pictures. Individual 7: top picture at age 4, bottom picture at age 32. Individual 8: at age 8.5 years and 10.3 years. Individual 10: at age 7. Individual 15: top picture, age 7; bottom picture, age 14. Individual 17: at age 14 in both pictures. Individual 16: at age 2 and 3, respectively. Individual 19: at age 5.7 years old. Individual 22: at age 8 years old.

vomiting. After another three months, she developed a life-threatening status dystonicus with rhabdomyolysis and fever, which included profuse sweating. Neuro MRI reported subcortical hyperintensities in the white matter and basal ganglia, some of them were reversible and some left a defect/cyst. At age of 14 years, operative spinal fusion was performed without postoperative complications. She is in a good clinical status now, has no pain (medicated with gabapentin), no vomiting

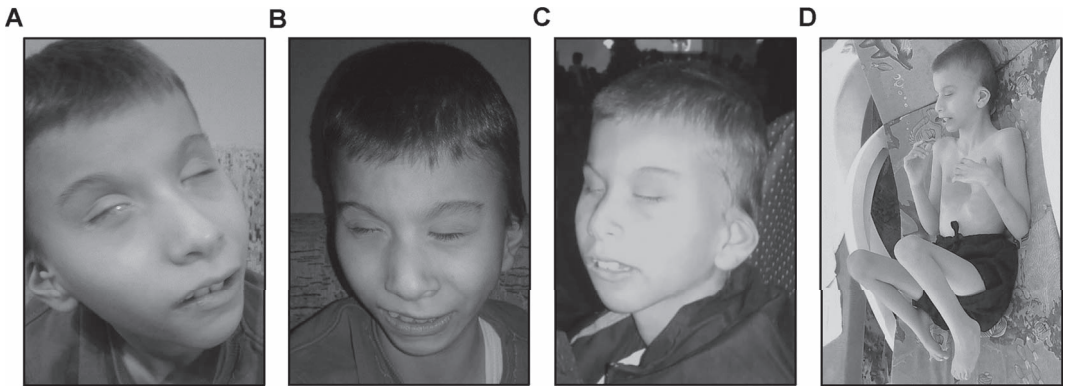

Figure 3. An individual with *NAA10* c.455_458delCTCA variant. At 11 years of age, presenting with microcornea, microphthalmos, pectus excavatum, clubfeet, syndactyly (on 2nd and 3rd digits of feet) and also mildly so on the 3rd and 4th digits of his fingers.

and acceptable dystonic movements. She is now wheelchair bound.

We also report a 10-year-old girl (Individual 18) with a *de novo* c.311C>A p.(Ala104Asp) variant (see Fig. 2). She was born full term from a normal pregnancy. She is diagnosed with global developmental delay, growth hormone deficiency, sensory processing disorder, ADHD (combined type), mixed receptive and expressive language disorder, hypotonia, fine motor delay, short stature, anxiety, astigmatism, anisometropia conjunctivae and sleep disorder. Her anxiety manifests with public avoidance, skin picking and stereotypies. Her clinical history was also significant for hip dysplasia, and she wore a pelvic harness for the first 6 weeks of life. She has no history of seizures. Cognitive testing reports ID, although testing is complicated by her ADHD. Additional information is provided in the Supplementary Material.

We identified two individuals with a recurrent c.361C>G p.(Leu121Val) variant. The first is a 6-year-old girl (Individual 19) with a *de novo* c.361C>G p.(Leu121Val) variant (see Fig. 2). Growth cessation occurred at week 37 gestational age, and she was born at 39.4 weeks via an emergent C-section. Her birth weight was 2.5 kg. Her HC was under 20th percentile until she was 3 years old and with growth is now just under 50th percentile. She was diagnosed with hip dysplasia at 9 months old and global developmental delay at 18 months old. She is non-verbal and has severe ID. She has mixed muscle tone. She did not start walking until she was 2 years of age. She was diagnosed with severe ASD at 3 years of age, lacks eye contact, becomes easily anxious, toe walks and engages in self-stimulatory behavior. A Neuro MRI performed at 2.5 years was normal. There are no cardiovascular issues and no sign of seizures. She is happy but has very little patience, challenging behaviors and struggles with sensory issues in new and loud environments. She has no feeding issues; however, she does not have the fine motor skills to feed herself. She cannot run (she skips instead) and cannot coordinate to use a bicycle. She has severe sleep issues. As an infant, she had silent reflux, which was resolved. She has normal weight and stature for her age.

The second individual with the c.361C>G p.(Leu121Val) variant is a 14-year-old female (Individual 20). She was first evaluated at 20 months for speech delay and possible hearing loss. She has significant receptive and expressive language delay, anxiety, avoidance behaviors, mild dystonia, fine and gross motor delays and borderline non-verbal abilities with adaptive abilities in the mildly delayed range. She is diagnosed with mild ASD. At age 12, she was diagnosed with moderate to profound ID. At age 13 years, she was identified as having an NAA10, c.361C>G p.(Leu121Val) mutation and a duplication on chromosome 7. She does not have feeding issues and eats independently. She attends school with the assistance of an aide. She receives support services for speech, hearing and physical therapies. Medication includes sertraline for anxiety. According to her mother, the girl sweats profusely. The family history includes two older siblings with speech articulation issues. The mother is a college graduate who teaches school.

We report a 1.5-year-old female (Individual 21) with a *de novo* c.384T>G p.(Phe128Leu) variant. There is no pre- or perinatal history available. Her mother states that early feeding problems were alleviated with the insertion of a gastric tube at 2 months of age. The child has gastric reflux and is successfully medicated with ranitidine. The mother states that the child's head growth such as HC and weight is less as compared to other girls the same age. The child has cortical vision impairment and does not make good eye contact. The child has delayed motor development, chorea, overriding toes and a single palmar crease. Neuro MRI exam reported bilateral pyramidal characteristics with deviations in the basal ganglia. The mother states that the child can roll from side to side if she is lying on her back. Hand usage is limited, but she actively moves her legs.

We report an 8-year-old girl (Individual 22) with a *de novo* c.440T>C p.(Met147Thr) variant (see Fig. 2) who has developmental delay, coordination issues, sensory processing disorder and self-stimulatory behaviors, but she is very social and there is no other evidence of ASD. Following intense speech therapy intervention, she now speaks a few words (~12). She can show testing in the near age-appropriate reading comprehension and has an above-age-level math ability when she can escape from her major sensory and behavioral impairments. Neuroimaging reports a thinning corpus callosum. She has microcephaly, stigmatism, cortical visual impairment, acne, body odor, adrenarche and is a light sleeper (so no hypersomnolence). There are no cardiac issues.

An 11-year-old boy with a maternally inherited frameshift variant c.455_458delCTCA p.(Thr152fs) was identified (Individual 23, Fig. 3). This variant is not present in gnomAD. His clinical features include agenesis of corpus callosum, craniosynostosis, severe ID, severe global developmental delay, growth delay, generalized hypotonia, microcornea and microphthalmia, scoliosis, pectus excavatum, equinovarus, craniosynostosis (corrected by surgery) and an atrial septal defect, with some rotation of the heart in the chest. He is severely underweight, at 17 kg (<1st percentile), with height of 140 cm (~25th percentile). He

Figure 4. Mild facial dysmorphology and feet images of two individuals with *de novo* *NAA15* missense variants. Individual 6: photos were at 1.75 years and at 6.25 years, respectively. Abnormality of the dentition, broad philtrum, high palate, hypertelorism, microcephaly, persistent open anterior fontanelle and tented upper lip vermilion noted. Feet appear normal. Individual 7: at the age 8.6 years, with prominent forehead, prominent nasal tip, triangular nose, mild retrognathism and mild hypermetropia. Feet malposition was treated with 1 year physiotherapy.

had hypospadias, which was surgically corrected, and also has syndactyly (webbing) on two digits (2nd and 3rd digits) on his feet with webbing mildly present on two digits (3rd and 4th fingers). Behaviorally, he can be stubborn and also aggressive at times toward his mother. There are no issues with chewing and swallowing, but he has a very low appetite and often refuses to eat. He has no speech, does not sleep well and is not toilet trained. He is immobile, as per parent report. The mother, who is a maternal carrier, finished high school and 3 years of college. She characterizes herself as an 'average student', who did not finish college after the birth of her child. She subsequently had two daughters (ages 6 and 9), who have not yet been tested for inheritance of the variant, but appear to be developing normally. The 6-year-old daughter had a ductus arteriosus and an atrial septal defect at birth, but both conditions were surgically corrected in the first few months of her life. The mother developed multiple sclerosis after the second childbirth but does not have any other health issues.

Clinical presentation of individuals with variants in *NAA15*

Individual 1 has a c.334G>A p.(Asp112Asn) variant, with an unknown inheritance pattern. This boy was 16.9 years old at his last assessment. He was born at 38 weeks gestation via an emergent C-section (due to breech position). Birth weight was 7.9 pounds. The mother's prenatal history is notable for placenta previa and first trimester mild bleeding but no other concerns. The boy was diagnosed with Asperger's syndrome at 8 years of age, with notable attention problems. He is apparently very intelligent for his age, and there is no other history of developmental or language delays. He walked at 12–14 months of age and began using 2-word sentences at 18 months of age. He was toilet trained at ~2 years of age. He was diagnosed with generalized epilepsy and had his first seizure episode at 6 years of age. He has had multiple abnormal EEGs, and his seizures are now well managed by medication. Neuro MRI results were normal. Height and weight have been somewhat below average but otherwise normal on the growth curves. He has a curved fifth finger on both hands. There is a history of mild fifth finger curving in his mother. He has mild constipation, and there are no other medical concerns.

Individual 2 has a *de novo* c.1014G>T p.(Lys338Asn) variant. The only available clinical information is that this individual has ASD.

Individual 3 is a 10-year-old female with a paternally inherited c.1348A>G p.(Lys450Glu) variant. She was born at 40 weeks via vaginal delivery with placental detachment. She has hypertelorism and a broad nasal bridge as well as behavioral problems including selective mutism and pervasive developmental disorder.

Individual 4 was age 12-year-old at his last visit, and he has a *de novo* c.1413A>C p.(Glu471Asp) variant. The child was diagnosed with ADHD, and there was concern of unclear speech. The patient had epileptic discharges over the left temporal region and occasionally the frontal central. MRI indicated mild, deep white matter, hyperintense signal changes.

Individual 5 is an 11-year-old female with a maternally inherited c.1424C>T p.(Ala475Val) variant. She was diagnosed with ASD (confirmed with Autism Diagnostic Observation Schedule (ADOS), Autism Diagnostic Interview (ADI) and clinical judgment using Diagnostic and Statistical Manual of Mental Disorders (DSM)-IV criteria). Her cognitive abilities fall into the extremely low range (verbal IQ = 36). Her parents report that her adaptive abilities were impaired (adaptive composite = 41). Abnormalities were first noted in her development at 12 months of age. She first used single words at 66 months and has not developed phrase speech.

Individual 6 was age 6.2 years old at her last assessment, and she has a *de novo* c.1450T>C p.(Cys484Arg) variant. At her initial presentation, she was 2 years and 8 months. At that age, she weighed 11 kg and was 80 cm tall, with an HC of 43 cm. She had global development delay, which was improved. Developmentally, she sat at 10–11 months and walked at 2 years.

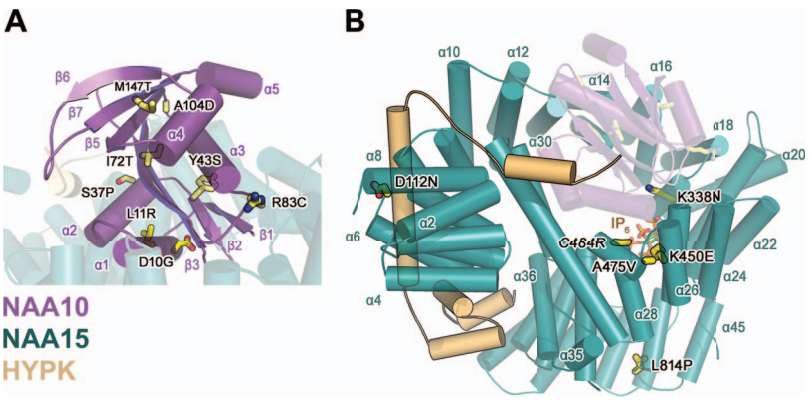

Figure 5. Annotated structure of human NatA/HYPK. (**A**) Missense variants (yellow; stick format) found in NAA10 (purple) and (**B**) NAA15 (dark teal) separately annotated on crystal structure of HYPK (light orange)-bound NatA (PDB: 6C95) in cartoon with bound IP_6 (brown; stick format).

Cognitively, she developed normally. She has facial dysmorphisms, abnormal dentition, broad philtrum, high palate, hypertelorism, microcephaly, persistent open anterior fontanelle and tented upper lip vermillion (Fig. 4). She is short for her age. She also had *café-au-lait* macules on each leg of the lower limbs and hypermobility of the digits. She also has a *de novo* c.1837C>T, p.(Arg613Cys) variant in *TCF12*, a gene previously associated with an autosomal dominant non-syndromic coronal craniosynostosis (20).

Individual 7 was 8.6-year-old at the last known visit, with a *de novo* c.2441T>C p.(Leu814Pro) variant. She has global development delay, language delay and fine motor difficulties. Developmentally, she walked at 26 months and spoke her first words at 18 months. Cognitively, she has mild to moderate ID. Wechsler Intelligence Scales for Children (WISC) testing reported scores of reasoning, 67; visuospatial, 57; speed, 60. Vineland II scores were communication, 30; daily life, 67; socialization, 82; motor skills, 60. Since 6 months old, she has had 6 febrile seizures, and since 6.5 years of age, she has had non-febrile seizures (absence), which were treated with ethosuximide. She has a prominent forehead and nasal tip, triangular nose and mild retrognathism (Fig. 4).

Biochemical analysis

Thus far, mutant NatA *in vitro* acetyltransferase activity has been measured with either *Escherichia coli*-expressed recombinant hNAA10 protein solubilized using a maltose-binding protein (MBP) tag (or other affinity tag) as a monomer (4–6,8,21) or also in the context of an immunoprecipitated NatA complex (11,12,21). Furthermore, studies have been conducted using a *Saccharomyces cerevisiae* model system (22,23). Protein stability of some variants has been measured in HeLa cells with cycloheximide-chase experiments (5,8,12). Herein, we have expressed and purified recombinant NatA complex from insect Sf9 cells, with this complex being comprised of human NAA10 and NAA15 (15,18). We introduced and tested many of the published and novel variants, which are shown on the recent crystal structure in Figure 5. The acetyltransferase activities of these variants, in the presence and absence of the regulatory binding partner, HYPK, are shown in Figure 6, along with the thermal stability of the NatA complex with and without these various variants (associated *P*-values in Supplementary Material, Tables S2 and S3, respectively).

Functional characterization of human NatA missense variants of NAA10

The following mutants (D10G, L11R, S37P, Y43S, I72T, R83C, A104D and M147T) were soluble and purified to homogeneity. A few of the variants (A87S, L121V and F128L) were only characterized clinically at a much later date and were thus not assessed biochemically for this study. We found that, except for R83C and M147T, alterations in the catalytic subunit caused a significant decrease in enzymatic activity (Fig. 6A; Supplementary Table S2). Particularly, the activity of residues that make important contributions to the integrity of the fold of the catalytic subunit resulted in the largest decrease (D10G, S37P and A104D). These protein changes likely alter numerous interactions including the loss of hydrogen bond interactions and the perturbation of hydrophobic pockets (Fig. 5). Similarly, L11R, Y43S and I72T likely promote changes in the hydrophobic surfaces that they occupy, but they do not promote larger-scale structural changes that would impede N_t-acetyltransferase activity. For example, while bulky, L11R can occupy other rotameric positions, allowing the accommodation of its long aliphatic chain so that it may find a favorable orientation. M147T, on the other hand, does not appear to have any effect on NatA catalytic activity. By contrast, R83C appears to enhance NatA activity. It may promote the formation of a disulfide bond with NAA15-C322, which could allow for improved positioning of acetyl-CoA for catalysis. Interestingly, previous studies with monomeric human NAA10 have demonstrated that $NAA10_{R83C}$ has a diminished catalytic capacity (5), which is consistent with our findings indicating that in the absence of NAA15, $NAA10_{R83C}$ would no longer benefit from the catalytic stabilization provided by $NAA10_{R83C}$ -$NAA15_{C322}$ disulfide bond formation.

We were surprised to find that when we supplemented the NatA mutant reactions with HYPK and re-evaluated their enzymatic activities, HYPK-mediated inhibition of wild-type (WT) NatA activity was potentiated, decreased or nullified depending on the specific variant (Fig. 6B; Supplementary Material, Table S2). M147T, which had no effect in the heterodimeric state, significantly decreased NatA activity upon addition of HYPK. D10G, Y43S, I72T and A104D also appeared to sensitize NatA to HYPK-mediated inhibition while L11R, S37P and R83C did not have a significant effect. In WT, the NAA15 α26–44 helical stalk serves as the primary point of tight binding for the NAA15–HYPK interaction. It is possible that L11R and S37P are stabilized in the HYPK-bound complex relative to other mutants due to packing-induced stabilization between the NAA15 helical stalk and either NAA10 α1 (L11R) or NAA10 α2 (S37P) helices. In

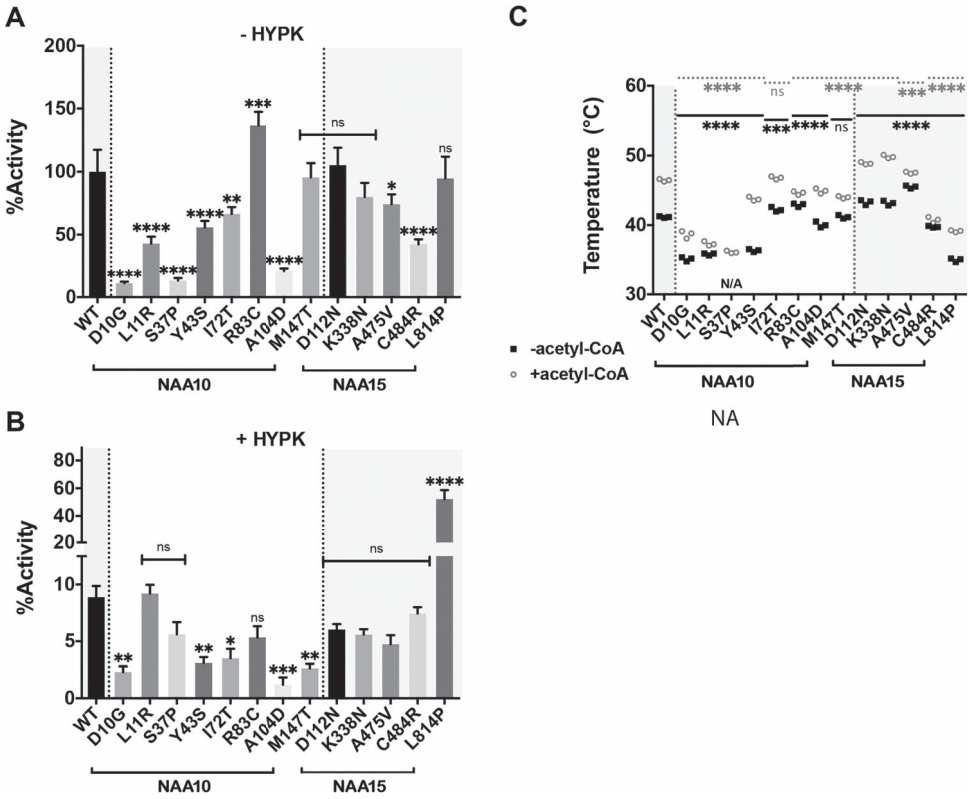

Figure 6. Comparison of NatA complex missense variants. Bar graph representing relative effect of a missense mutant compared to the heterodimeric WT complex (-HYPK) on (**A**) NatA complex activity and (**B**) NatA/HYPK complex activity. In both cases, activity was normalized with respect to WT NatA (-HYPK). Assays were performed in triplicate; error bars, SD. Significance was calculated relative to WT using Sidak's multiple comparisons test. (**C**) DSF evaluation of WT and mutant NatA variants (-HYPK). Assays were performed in absence (black squares) and presence of acetyl-CoA (gray circles). Assays were performed in triplicate with each replicate presented in a staggered scatter plot. Significance was calculated with respect to the complex assayed in the absence of acetyl-CoA (black line) or in the presence of acetyl-CoA bound (gray dotted line) using Sidak's multiple comparisons test. ****$P \leq 0.00001$; ***$P \leq 0.0001$; **$P \leq 0.001$; *$P \leq 0.05$; Not significant (ns) $P > 0.05$.

contrast, HYPK binding nullified the enhancing effects of R83C due to the HYPK-induced conformational changes in the acetyl-CoA binding pocket.

Next, we compared the thermostability of heterodimeric NatA complexes with mutant heterodimeric complexes in the absence and presence of its cofactor, acetyl-CoA, using differential scanning fluorimetry (DSF) (Fig. 6C; Supplementary Material, Table S3). We found that all of the missense changes, except I72T, R83C and M147T, were destabilized in the absence of cofactor when compared to WT. By contrast, all changes, except I72T, were destabilized in the presence of acetyl-CoA with respect to WT. These results indicate that the missense changes are overall destabilizing for the heterodimeric complex, where changes that destabilize the GNAT fold—such as S37P, D10G, L11R, Y43S and A104D—reduce the stability of the complex in the absence as well as the presence of acetyl-CoA. On the other hand, I72T may play a minor role in stabilizing the apo-state of the mutant complex where the smaller side chain promotes the compaction of the hydrophobic pocket between the NAA10 β4-strand and α3 helix. The stabilization of the R83C mutant complex likely is a result of the formation of a disulfide bond with NAA15-C322. By contrast, the R83C complex is likely no longer able to fully benefit from the acetyl-CoA stabilizing effects due to the loss of electrostatic interaction between the positively charged Arg83 side chain and the negatively charged phosphodiester acetyl-CoA backbone. Similarly, M147T likely diminishes the packing between the α4 helix and β7-strand, diminishing the stabilizing hydrophobic packing effects of acetyl-CoA binding.

Functional characterization of human NatA missense variants of NAA15

Except for K450E, all the variants biochemically tested (D112N, K338N, A475V, C484R and L814P) were soluble and were purified to homogeneity, while one variant (E471D) was only characterized clinically at a much later date and was thus not assessed biochemically for this study. We found that K450E appeared to break the NatA heterodimeric complex, causing $NAA15_{K450E}$ to elute throughout the S200 column rather than as a single peak (Fig. 7). Since K450 makes important interactions with the structural inositol hexaphosphate (IP_6) molecule, we reasoned that K450E would result in the loss of a hydrogen bond as well as introduce a charge–charge repulsion between the mutant residue and the negatively IP_6 phosphate moieties. Consistent with this possibility, we found that we could rescue the NAA10–NAA15 association and enzymatic activity when the complex was prepared with 15 μM IP_6, as documented in (24), suggesting that the K_D for the IP_6–NatA complex interaction may be decreased in the K450E variant (Fig. 7; Supplementary Material, Table S4). Consistent with the overall destabilization of the complex, due to an enduring charge–charge repulsion and the loss of a hydrogen bond interaction, we observed that the additional IP_6 did not improve the melting temperature of the $NAA15_{K450E}$ mutant complex (Fig. 7; Supplementary Material, Table S5).

To understand how the other NAA15 missense changes impacted NatA complex activity and thermostability, we

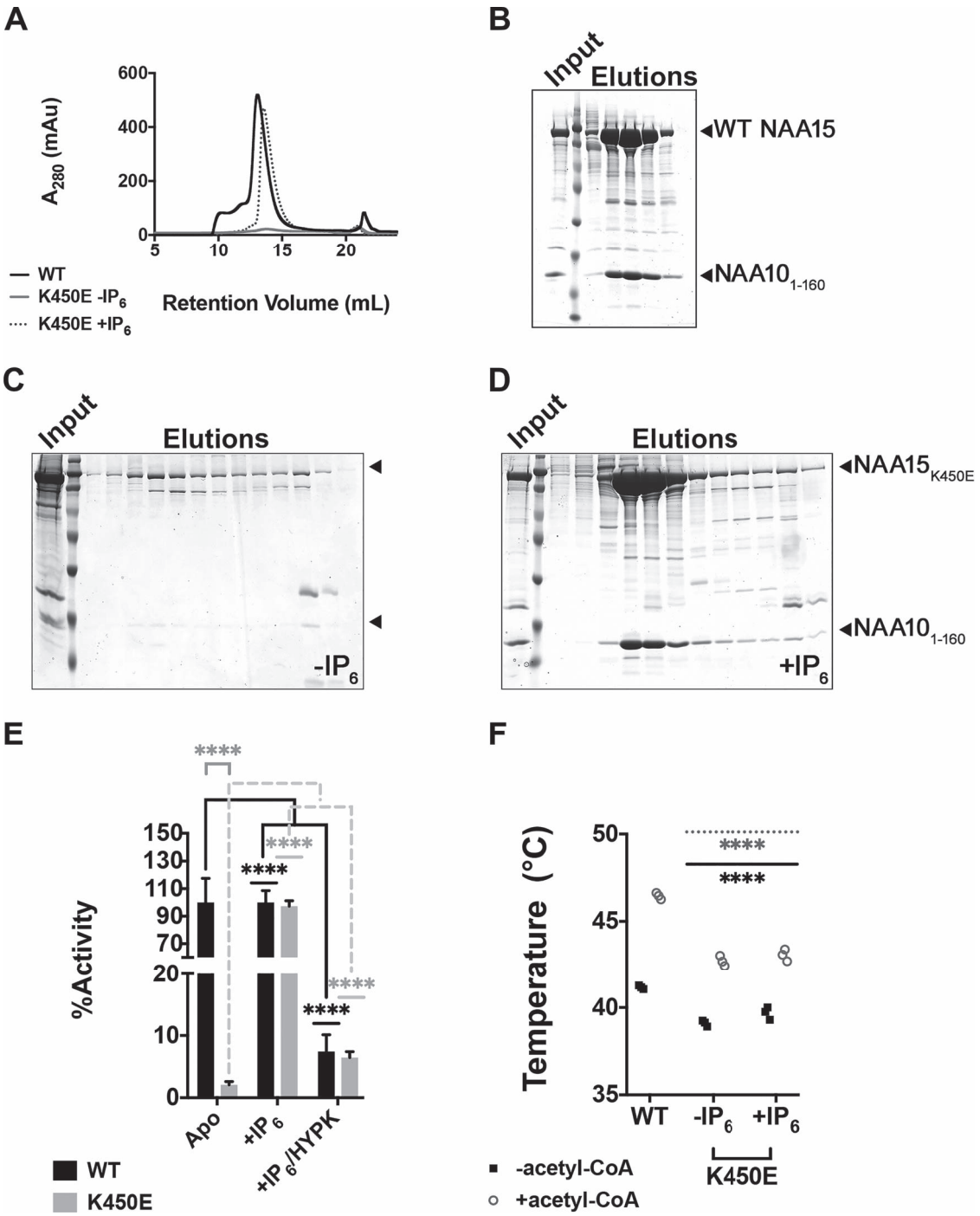

Figure 7. IP_6 partially rescues $NAA15_{K450E}$ complex function. (**A**) S200 gel filtration chromatogram comparing WT (solid black line) and HIS-$NAA10_{1–160}$/$NAA15_{K450E}$ (K450E) mutant prepared without (solid gray line) and with 15 μM IP_6 (dotted gray line). (**B**) Corresponding SDS-PAGE gel to the WT S200 elution profile for A. (**C**) Corresponding SDS-PAGE gel to the K450E complex $–IP_6$ elution profile for A. (**D**) Corresponding SDS-PAGE gel to the K450E complex $+IP_6$ elution profile for A. (**E**) Bar graph representing relative effect of K450E (gray) variant with respect to the heterodimeric WT (black) complex on NatA complex activity, when prepared without (Apo) or with IP_6 ($+IP_6$), as well NatA/HYPK complex ($+IP_6$/HYPK) activity. Activity was normalized with respect to WT NatA (Apo). Assays were performed in triplicate; error bars, SD. Significance was calculated relative to WT using Sidak's multiple comparisons test. (**F**) DSF evaluation of WT and K450E. K450E was evaluated in the absence ($–IP_6$) and presence of IP_6 ($+IP_6$). Both WT and K450E DSF assays were performed in absence (black squares) and presence of acetyl-CoA (gray circles). Assays were performed in triplicate with each replicate presented in a staggered scatter plot. Significance was calculated either with respect to the WT in the absence of acetyl-CoA (black line) or in the presence of acetyl-CoA (gray dotted line) using Sidak's multiple comparisons test. ****$P \leq 0.00001$; ***$P \leq 0.0001$; **$P \leq 0.001$; *$P \leq 0.05$; ns $P > 0.05$.

characterized the overall effect of these variants on NatA activity—in the absence and presence of HYPK—and performed DSF assays in the absence and presence of acetyl-CoA. We found that D112N and K338N both did not significantly impact N_t-acetyltransferase activity (Fig. 6A and B; Supplementary Material, Tables S2 and S3), likely due to the role and position of D112 as a surface residue and K338 as a residue that is distantly located from the NAA10-NAA15 interface (Fig. 5B). However,

D112N and K338N did appear to stabilize the complex with respect to WT, in the absence of acetyl-CoA, which was also the case for all of the NAA15 missense changes (Fig. 6C). K338N may serve to form new hydrogen bond interactions, which may stabilize the complex. A475V and C484R had reduced N_t-acetyltransferase activity in the absence of HYPK, and, interestingly, L814P had increased N_t-acetyltransferase activity in the presence of HYPK, though it maintained its ability to interact with HYPK (Fig. 6A and B; Supplementary Material, Fig. S1). As a heterodimeric complex, C484R results in a significant reduction in NatA activity due the inherent steric bulk of the Arg side chain. In the case of A475V, the Val side chain, while larger than the WT Ala residue, likely contributes just enough to a small shift in the NAA15 α26 helix packing against the NAA10 α1 and α2 helices, shifting the helices so that the complex catalyzes activity less efficiently. These mutant-induced steric shifts, however, are nullified upon HYPK binding, likely due to the stabilizing effect of $HYPK_{UBA}$ (C-terminal) binding to the NAA15 metazoan-specific C-terminus (Fig. 6A and B).

A475V, C484R and L814P were found to all likely impact the stability of the NAA10–NAA15 interface through the stalk of helices (α26–45), depending on whether or not acetyl-CoA is bound to the mutant complex (Fig. 6C). Although A475V and C484R are located in the same area of the NAA15 helical stalk, these missense changes have different effects on the thermostability of the NatA complex (Fig. 6C). This difference likely arises from the positioning and identity of the variants: they are on opposite ends of the same α26 helix and are steric opposites. In the case of C484R, the bulky Arg variant located near the NAA10 α1/α2 helices potentially pushes away NAA15 α26, resulting in diminished NAA10–NAA15 contact area. A475V likely minimally perturbs NAA15 α26 so that it may pack more closely with the NAA10 α1/α2 helices. A larger residue in this position, however, would likely lead to a similar effect that is observed with C484R. In contrast, L814P has no effect on NatA complex activity unless HYPK is bound (Fig. 6A and B), likely due to the steric restraints generated by a Pro substitution, reducing HYPK binding integrity and, therefore, the inhibitory capacity of the interaction. Unsurprisingly, the L814P mutant reduces the thermostability of the complex, regardless of the binding of acetyl-CoA (Fig. 6C). This data is consistent with a model where the L814P variant results in a dramatic reduction in the dynamics of the NAA15 α26–45 helical stalk, which is necessary for the clamp-like binding of HYPK binding as well its intrinsic NatA inhibitory activity.

Discussion

The amino acid changes D10G, S37P and A104D in NAA10 were shown to have very low NatA acetyltransferase activity in the absence of HYPK (Fig. 6). The variants L11R, Y43S and I72T also have activity that is lower than WT in the absence of HYPK but not nearly as low as the D10G, S37P and A104D changes. The overall activity of WT NatA is substantially decreased in the presence of HYPK (15). However, in the presence of HYPK, the variants that are significantly less active than WT are D10G, Y43S, I72T, A104D and M147T, although the overall activity of the WT enzyme is itself only at ∼10% of the activity seen without HYPK (see *y*-axis) and thus the signal-to-noise ratio is also lessened. The results in the absence of HYPK are more consistent with the observation that males with the D10G variant (reported herein) and S37P variants (4) are very severely affected (and have very similar facial features), whereas males with the Y43S variant can live to adulthood (8). Furthermore, boys with the I72T variant are also not as dysmorphic (see Fig. 2), and the two brothers in one family were 5.5 and 8.5 years old, respectively, at the time of that report (11). It is notable that the individual in the second family with the I72T variant (Individual 3 in Table 1) died suddenly in January 2018 due to cardiopulmonary issues, likely due to complications from the cardiomyopathy. It is uncertain, however, if there was an arrhythmia event that preceded this decompensation, and an autopsy was not performed. The difference in severity between the S37P and the I72T variant is further demonstrated in Figure 8, Table 3 and Supplementary Material, Table S6, in which the acetyltransferase activity, in addition to the thermostability (Fig. 6), of the S37P variant is considerably lower than the I72T variant. To date, we are not aware of any known males with A104D or L11R variants, but the prediction based on these functional studies is that the A104D variant would be more severe than the L11R variant, although both variants would have a major impact on the quality of life. It is interesting to note that the M147T variant in NAA10 only has decreased NatA acetyltransferase activity in the context of the NatA/HYPK complex (Fig. 6B versus Fig. 6A). In conjunction with the thermostability data showing only decreased stability in the presence of acetyl-CoA (Fig. 6C), this suggests that the reduction in NatA/HYPK activity arises from a diminished ability to bind to the acetyl-CoA cofactor. HYPK has been demonstrated to improve the acetyl-CoA K_M of WT NatA through a shift in the acetyl-CoA binding pocket (15). Due to the inherent difference in size between Met and Thr, mutation of Met147 to Thr would reduce the effect of HYPK binding, thus impacting the overall activity and stability of NatA in the presence of HYPK and acetyl-CoA, respectively. This further demonstrates the utility and superiority of conducting these *in vitro* assays with NatA and NatA/HYPK as opposed to with Naa10 alone.

The phenotype of a female heterozygous for an *NAA10* disease-contributory variant can range from asymptomatic to having some of the same clinical findings as affected males, including a range of ID and cardiac findings, depending on specific variants and presumed favorable versus non-favorable X-chromosomeinactivation (XCI). Skewed XCI in B cells in female carriers of different *NAA10* disease-associated variants has been observed, but the direction of skewing was not demonstrated in many cases, making it very difficult to speculate about the impact of X-chromosome skewing on the phenotypic expression in those individuals. In addition, it is possible that X-chromosome skewing can occur in different ratios in different tissues, particularly if expression of the protein from the mutated X-chromosome confers either a growth advantage or disadvantage in specific tissues. Although one group did report a significant correlation ($r(s) = 0.51$, $P = 0.035$) between XCI values for blood and/or spleen and brain tissue (25), the sample size was small and there was substantial scatter in their data. It is certainly the case that some female carriers of these variants are much less affected (if at all) with cognitive disabilities. The carrier mothers in the Ogden syndrome family with c.109T>C p.(Ser37Pro) were never diagnosed with ID or any other serious medical condition. It was previously shown that their XCI was nearly completely skewed toward the WT allele in blood (21), and it is possible that this might have been true in other tissues of their bodies as well. Although it was reported that the carrier mother with c.128A>C p.(Tyr43Ser) might have had a 'learning disability' or 'learning problems' when compared to her siblings (8), the mother reports that she finished her formal education and was gainfully employed, and there is no documented evidence for ID or learning disability, and there was never any formal IQ testing. The maternal carrier in Family 3 with c.215T>C p.(Ile72Thr) completed college and was

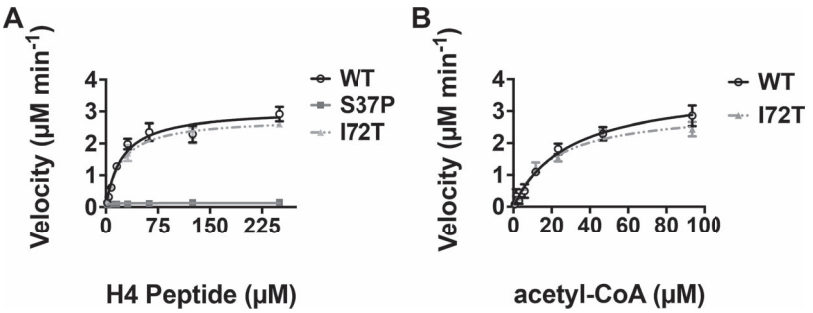

Figure 8. NAA10 mutant enzyme kinetics. Michaelis-Menten kinetics of WT and catalytic mutant NatA complexes with respect to (A) H4 (B) acetyl-CoA. Assays were performed in triplicate; error bars correspond to the SD for each point.

Table 3. Naa10 mutant kinetic parameters

Mutant	Substrate	k_{cat} (min^{-1})	K_M (μM)	k_{cat}/K_M (μM min^{-1})
WT	H4	310 ± 13.3	23 ± 3.3	13 ± 0.2
S37P		13 ± 0.9****	1.9 ± 0.8****	6.6 ± 0.4****
I72T		280 ± 8.8 (ns)	22 ± 2.3 (ns)	13 ± 0.1 (ns)
WT	Acetyl-CoA	380 ± 24	29 ± 4.5	13 ± 0.2
I72T		310 ± 14*	21 ± 2.5 (ns)	15 ± 0.1***

Michaelis–Menten parameters, corresponding to Figure 8A and B, of WT catalytic mutant NatA complexes with respect to H4 or acetyl-CoA. Error bars correspond to the standard deviation for each point. $n = 3$.

gainfully employed. She did have test-related anxiety during schooling and did receive math tutoring, but she did not have any formal IQ testing nor was she diagnosed with an intellectual or learning disability. One major problem in the field is that many female carriers have not had systematic IQ testing, so a quantitatively reliable way to compare and contrast them does not currently exist. Considering this, we recommend that future studies should include systematic IQ testing of female carriers.

It is surprising that the R83C variant has increased (not decreased) NatA acetyltransferase activity in the absence of HYPK, and it does not exhibit any significant difference in NatA acetyltransferase activity in the presence of HYPK (Fig. 6A and B). This variant also has only slightly decreased thermal stability compared to the WT NatA complex, and it is not nearly as destabilized as some of the other NAA10 variants (D10G, L11R and S37P) (see Fig. 6C). These results differ from the decreased activity that was reported when testing acetyltransferase activity of monomeric NAA10 with peptides starting with EEEI-, DDDI- and SESS-. There is only one reported male hemizygous for the R83C variant who died in the first week of life with supraventricular tachycardia, pulmonary hypertrophy, mild ventricular hypertrophy and diffuse small cortical kidney cysts. Brain imaging was not reported, so it is unknown whether he had any hydrocephaly (5). The R83C variant may promote the formation of a disulfide bond with NAA15 C322. In the absence of acetyl-CoA, this change can promote a minor stabilization of the NatA mutant complex. However, the binding of acetyl-CoA to the mutant NatA complex does not impart the same level of stabilization as in WT due to the loss of the electrostatic interaction with the acetyl-CoA phosphodiester backbone in addition to the restricted conformation. Overall, when considering the activities of the monomeric NAA10 versus dimeric NatA complex, the monomeric mutant NAA10 is reported to be less active for S37P and R83C (4,5). By contrast, in the case of the heterodimeric complex NatA, S37P exhibits reduced activity while R83C exhibits an enhanced activity (likely afforded by the disulfide bond formation with NAA15). This suggests that the phenotype of individuals with the R83C may manifest through a different mechanism of action than the other missense variants, which seem to be entirely hypomorphic, at least as related to canonical acetyltransferase catalytic activity. There is a wide spectrum among individuals with *NAA10*-related disorder with regard to number of findings and severity of phenotype. Males with *NAA10*-related syndrome may have symptoms at different ages; those with arrhythmias or other serious cardiac conditions may be embryonic lethal, while others are apparent at birth with cardiac concerns, hypotonia and dysmorphic features, and others come to attention later with relatively non-specific developmental/intellectual and growth impairments. The current results reveal that the various variants have different effects on the overall NatA acetyltransferase activity and complex stability, which can also certainly have a major effect on disease outcome.

Prior studies report that NAA10 I72T is destabilized, while binding to NAA15 most likely is intact (11). That study concluded that the NatA activity of NAA10 I72T appeared normal while its monomeric activity was decreased (11). Our current results contradict this and suggest that the NatA activity of NAA10 I72T is decreased, in the presence and absence of HYPK, but that the stability of the NatA complex was unaffected. This result seems to be more consistent with the phenotypic presentation of the probands with NAA10 I72T variants.

When a variant occurs *de novo* in an affected proband, this is itself a piece of evidence in favor that the variant is likely contributing to the phenotype of interest (as a PS2 in the American College of Medical Genetics (ACMG) criteria) (26), so the *de novo* variants reported herein are classified as pathogenic, based on the following ACMG criteria: (1) PS2—*De novo* (both maternity and paternity confirmed) in a patient with the disease and no family history; (2) PS3—Well-established *in vitro* functional studies supportive of a damaging effect on the gene or gene product; (3) PM1—Located in a mutational hot spot and/or critical and well-established functional domain (e.g. active site of an enzyme) without benign variation; (4) PM2—Absent from

controls (or at extremely low frequency if recessive) in Exome Sequencing Project, 1000 Genomes Project or Exome Aggregation Consortium; and (5) PP2—Missense variant in a gene that has a low rate of benign missense variation ($Z = 2.41$ for *NAA10* and $Z = 3.81$ for *NAA15* in gnomAD v.2.1.1) and in which missense variants are a common mechanism of disease (26).

For those variants presented herein that are inherited from a parent and are thus not *de novo*, additional individuals with the exact same variants should be identified in the future to provide further evidence for their contribution to the phenotypes of interest. For now, we classify these variants as likely pathogenic, based on the same ACMG criteria but excluding the PS2 *de novo* criteria (26). Although all of the variants in *NAA15* were shown to affect either NatA activity or complex stability, the variant D112N has an unknown inheritance pattern, K450E has paternal inheritance and A475V has maternal inheritance. We note that two of the inherited variants in *NAA15*, K450E and A475V, were also found to be present at a very low frequency in gnomAD (once for K450E and twice for A475V), so the above PM2 criteria cannot be used for those two variants, given that *NAA15* is autosomal, whereas very low-frequency variants in *NAA10* would be eligible, as those are X-linked recessive (26). As such, these two parentally inherited variants in *NAA15*, K450E and A475V, only meet the ACMG criteria of PS3, PM1 and PP2, which nonetheless still classifies them as likely pathogenic, based on '1 Strong (PS1–PS4) AND 1–2 moderate (PM1–PM6)' (26). There is clearly variable expressivity, however, as the father with the K450E variant was never diagnosed formally with any ID or ASD, although there was some question of whether he may or may not be mildly affected. There is no information available for the mother with the A475V variant. This issue of variable expressivity was also found with truncating variants in *NAA15* (16), so it is not surprising to find this also for missense variants; however, we fully acknowledge that the support for pathogenicity is somewhat weak for these two inherited variants. Additional families will need to be identified with these exact same variants in order to help prove or disprove their disease contribution, and future studies of patient-derived cell lines could also help to further prove the pathogenicity of these variants.

The boy (Individual 23) with the maternally inherited frameshift variant c.455_458delCTCA p.(Thr152Argfs*6) in *NAA10* has many phenotypic features that are shared with the previously reported family with LMS with a mutation in the intron 7 splice donor site (c.471+2T>A) of *NAA10* (13). This most notably includes the microphthalmia, severe ID, scoliosis and syndactyly. This variant is not present in gnomAD, and there are only two other truncating variants present in gnomAD in the canonical NAA10 transcript, namely p.Ser228Ter and p.Ser233Ter, with the former being present only one time in a heterozygous female and the latter variant being present three times (one time in a heterozygous female and two times in hemizygous males). The canonical transcript of *NAA10* encodes a protein that is only 235 amino acids in length, so these two truncating variants in gnomAD occur at the very C-terminus of the protein, thus likely having no functional effect, whereas p.(Thr152Argfs*6) removes the C-terminus of NAA10, but leaves the acetyltransferase domain intact (Fig. 1). It was previously shown that the mutation in the intron 7 splice donor site (c.471+2T>A) generated a very small amount of truncated NAA10 protein, which could have had residual NatA activity, although it was also shown that this protein likely aggregates in the cytoplasm (13). Although some of the individuals with missense changes in NAA10 have milder eye or visual anomalies, including astigmatism, cortical visual impairment, hyperopia and/or myopia, none of them have microcornea or microphthalmia. Even if any truncated NAA10 protein has NatA activity, the overall level of this activity should be much less due to its much lower expression level (13). The expression level for the frameshift variant c.455_458delCTCA p.(Thr152Argfs*6) is presumably also substantially less, likely due to nonsense-mediated decay of the messenger RNA, although there are currently no patient-derived cells from this proband available to test this hypothesis.

From a mechanistic perspective, it is worth noting that our identification of a frameshift variant in the C-terminal region of NAA10 could be explained instead by loss of activity of some function associated with the C-terminal region. Although the serine residue at position 209 (Ser209) in NAA10 was shown to be a phosphorylation site of IKK-β, leading to the destabilization of NAA10 and its proteasome-mediated degradation (27), the absence of this IKK-β phosphorylation site in any truncated protein would be predicted to increase, not decrease, the protein levels of the truncated protein. Also, it has been reported that the C-terminus of NAA10 is required for interaction with TSC2, an inhibitor of the mTOR (mammalian target of rapamycin) pathway (28). After forming a complex with TSC2, NAA10 acetylates TSC2, both stabilizing TSC2 and increasing its cellular concentration (28); therefore, NAA10 may play a role in the regulation of the mTOR pathway, which could be disrupted with loss of the C-terminal region.

It was previously shown by quantitative real-time Polymerase Chain Reaction (PCR) analysis in the fibroblasts of three affected male individuals with LMS that the level of *STRA6* expression was significantly reduced, in comparison to controls, which suggested that these individuals may have retinol uptake deficiencies (13). Several studies had shown that cellular uptake of vitamin A/retinol from its RBP4-bound form is dependent on the membrane receptor protein, STRA6 (29,30), and it was then demonstrated that these same three individuals (VI-9, VI-10 and VI-11) in the LMS family had deficiencies in retinol uptake (13). These results suggested that *NAA10* may play a role in the retinoic acid signaling pathway and in normal eye development.

In conclusion, we have presented phenotypic information on some new variants in *NAA10* and *NAA15*, including one frameshift variant in *NAA10* associated with microphthalmia, along with additional phenotypic information on some previously published *NAA10* variants. Biochemical analyses have suggested some possible explanations for the phenotypic differences among these variants, although it remains an open question why reduced expression and/or truncation of NAA10 can result in microphthalmia, whereas missense changes have not been shown to be associated with microphthalmia.

*Note. While this manuscript was under review, 3 families, including 15 affected individuals with syndromic X-linked microphthalmia, were reported in which hemizygous *NAA10* polyadenylation signal variants segregated with the disease and were absent from gnomAD. Quantitative PCR and RNAseq showed ~50% reduction of *NAA10* mRNA levels and also abnormal 3′ untranslated regions (UTRs) in affected individuals (31).

Materials and Methods

Clinical features methodology

Phenotypic information was collected through clinicians and/or directly from families with missense or frameshift variants in *NAA10* and from families with missense variants in *NAA15*. New

families were identified via a world-wide collaboration between multiple institutions, via social media, or through GeneMatcher, a web-based tool for connecting researchers with an interest in the same gene (32). All families had been referred for the investigation of idiopathic developmental delay and ID. Several individuals were identified through the Deciphering Developmental Disorders study. The study was performed in accordance with protocols approved by the institutional review boards of participating institutions. Phenotypic information was obtained from clinical records with varying amounts of available data, ranging from a list of the key clinical features to detailed history and examination findings. Written informed consent was obtained for publication of photographs, and these photographs were reviewed by one medical geneticist (A.R.) to assign dysmorphic features in a systematic manner.

Detailed clinical summaries for each subject are provided in Supplementary Material, File S1. Both pertinent positive and negative features were noted, with phenotypes classified as 'pertinent negatives' only if the provided clinical information explicitly stated that a phenotype was denied by the parents, was noted to be absent during physical examinations or not reported during diagnostic procedures. Clinical features were only reported as pertinent negatives if this was explicitly mentioned in the records; otherwise, these were classified as 'unknown' or 'not available'. The relative prevalence of each phenotype was calculated by dividing the number of individuals positive for the phenotype by the sample size. Percentiles for HC, weight and height were calculated using CDC growth charts.

Variant identification and bioinformatics methodology

Variants were identified using exome sequencing primarily through clinical diagnostic testing. The sequencing kits and technology varied based on the different companies involved, and the variants of interest were highlighted in the clinical diagnostic test reports.

Construction of *E. coli* expression vectors

A pET-m41 vector engineered to contain an N-terminally MBP-tagged HYPK was kindly donated to us by Thomas Arnesen (University of Bergen).

Construction of baculoviruses

A plasmid containing the WT hNatA was generated using a pFastBac dual vector engineered with a C-terminal truncation construct coding for the human $NAA10_{1–160}$ and a non-cleavable 6xHis-tagged full-length NAA15 (866 residues). Individual mutations were introduced using the Stratagene QuikChange protocol: $NAA10_{D10G}$ (GGT), $NAA10_{L11R}$ (CGC), $NAA10_{S37P}$ (CCC), $NAA10_{I72T}$ (ACC), $NAA10_{R83C}$ (TGC), $NAA10_{A104D}$ (GAC), $NAA10_{M147T}$ (ACT), $NAA15_{D112N}$ (AAT), $NAA15_{K338N}$ (AAT), $NAA15_{K450E}$ (GAA), $NAA15_{A475V}$ (GTA), $NAA15_{C484R}$ (AGG) and $NAA15_{L814P}$ (CCC). Mutagenesis of the WT plasmid was performed by BioBasic to generate the $NAA10_{Y43S}$ mutation (TCC). For each of these constructs, a bacmid was generated by transposition into DH10 bac competent *E. coli* cells using the bac-to-bac system (Invitrogen, Carlsbad, CA). *Spodoptera frugiperda* (Sf9) cells cultured in SFM II medium were transfected with the bacmid using cellfectin reagent (Invitrogen). The resulting baculovirus was amplified until reaching a high titer.

Expression and purification of WT and mutant 6xHis-tagged NatA constructs

Sf9 cells were grown to a density of 1×10^6 cells/ml and infected using the amplified WT $NAA10_{1–160}$/NAA15 baculovirus to a multiplicity of infection of ~1–2. The cells were grown at 27°C and harvested 48 h post-infection. All subsequent purification steps were carried out at 4°C. Cells were isolated by centrifugation and lysed in lysis buffer containing 25 mM Tris, pH 8.0, 500 mM NaCl, 10 mM imidazole, 10 mM β-mercaptoethanol (β-ME), 10 μg/ml phenylmethanesulfonyl fluoride (PMSF), DNase and complete, EDTA-free protease inhibitor tablet (Roche, Basel, Switzerland). The lysate was clarified by centrifugation and incubated with nickel resin (Thermo Fisher Scientific, Waltham, MA) for 1 h before washing the resin with ~125 column volumes (CVs) of lysis buffer and then eluted with 10 CVs of elution buffer (25 mM Tris, pH 8.0, 500 mM NaCl, 200 mM imidazole, 10 mM β-ME) by batch elution. Eluted protein was diluted to a final salt concentration of 200 mM NaCl and loaded onto a 5 ml HiTrap SP ion-exchange column (GE Healthcare, Chicago, IL). The protein was eluted in the same buffer with a salt gradient (200 mM–1 M NaCl) over the course of 20 CVs. Peak fractions were pooled, concentrated to a volume of 500 μl (100 kDa concentrator) and loaded onto and run on a Superdex 200 Increase 10/300 GL gel filtration column in sizing buffer containing 25 mM HEPES, pH 7.0, 200 mM NaCl and 1 mM TCEP. Peak fractions were pooled, concentrated to ~1–2 mg/ml (measured by UV_{280} by Nanodrop), and flash-frozen for storage at −80°C until use. Mutant NatA proteins were prepared as described for the WT NatA with the following exception. Lysis and all purification steps of $NAA10_{1–160}$/$NAA15_{K450E}$ were performed in the presence and absence of 15 μM IP_6 (Sigma) and analyzed by radioactive acetyltransferase assay (described below).

Expression and purification of MBP-tagged HYPK

MBP-tagged HYPK was expressed in Rosetta (DE3) pLysS competent *E. coli* cells. Cells were grown in Lysogeny broth (LB) media at 37°C to OD_{600}– 0.6–0.7 prior to inducing protein expression with 0.5 mM isopropyl β-D-1-thiogalactopyranoside at 18°C for ~16 h. All subsequent purification steps were carried out at 4°C. Cells were isolated by centrifugation and lysed in lysis buffer containing 25 mM Tris, pH 8.0, 150 mM NaCl, 10 mM β-ME, 10 μg/ml PMSF and DNase (Invitrogen). The lysate was clarified by centrifugation and incubated with amylose agarose resin (New England Biolabs, Ipswich, MA) for 1 h before washing the resin with ≥80 CVs of lysis buffer and then eluted with 10 CVs of lysis buffer supplemented with 20 mM maltose by batch elution. Eluted full-length and truncated MBP-HYPK constructs were loaded onto a 5 ml HiTrap Q ion-exchange column (GE Healthcare). The protein was eluted in the same buffer with a salt gradient (150 mM—1 M NaCl) over the course of 20 CVs. Peak fractions were pooled and dialyzed overnight into buffer containing 25 mM HEPES, pH 7.0, 200 mM NaCl and 1 mM Tris(2-carboxyethyl)-phosphine hydrochloride (TCEP). Dialyzed protein was concentrated to ~20–40 mg/ml by UV_{280} (Nanodrop 2000; Thermo Fisher Scientific) and flash-frozen for storage at −80°C until use.

Acetyltransferase assays

Human NatA acetyltransferase assays, in the presence or absence of HYPK, were carried out in 100 mM HEPES, pH 8.0, 50 mM NaCl 2 mg/ml BSA, where reactions were incubated with 10 nM of 6xHis-tagged human NatA alone (WT or mutant)

or mixed with 5 μM MBP-HYPK in a 30 μl reaction volume containing 50 μM each of substrate peptide and [^{14}C]acetyl-CoA (4 mCi/mmol; PerkinElmer Life Sciences, Waltham, Massachusetts) for 12 min at 25°C. The substrate peptide used in the assay corresponds to the first 19 residues of human H4 (GenScript, Piscataway, NJ), which was selected because it did not generate a substrate inhibition kinetic profile. $NAA10_{1–160}$/$NAA15_{K450E}$ purified in the absence (-IP_6) and presence of 15 μM (+IP_6) was utilized in the assay without additional IP_6. In the case of the latter sample, this resulted in a final concentration of ∼1.5 μM IP_6 after reaction setup.

To determine steady-state catalytic parameters of WT, $NAA10_{1–160/S37P}$/NAA15 and $NAA10_{1–160/I72T}$/NAA15, a saturating concentration of radiolabeled [^{14}C]-acetyl-CoA (100 μM) was incubated at 7 different concentrations of the H4 substrate peptide (ranging from 3.9–250 μM). Additionally, the acetyl-CoA K_m values of WT and $NAA10_{1–160/I72T}$/NAA15 were determined by titration of the acetyl-CoA at 8 different concentrations (ranging from 0.73–94 μM) in the presence of 350 μM substrate peptide. GraphPad Prism, version 5.01, was used for all data fitting to the Michaelis–Menten equation.

Thermal stability assays

Frozen aliquots of WT and mutant NatA proteins (in the absence of HYPK) were thawed and diluted in size exclusion buffer (25 mM HEPES, pH 7.0, 200 mM NaCl, 1 mM TCEP) to a final concentration of ∼0.94 μM (∼0.13 mg ml^{-1}). A total of 16 μl was added to the selected wells of a MicroAmp Optical 384 well plate (Applied Biosystems, Foster City, CA) to a final concentration of ∼0.75 μM (∼0.1 mg ml^{-1}). Sypro Orange (5000× stock, Thermo Fisher Scientific) was diluted 1:500 using size exclusion buffer, and 4 μl of that diluted stock was added to each well. The plate was spun down and heated from 20–95°C using a quantitative polymerase chain reaction (qPCR) (ABI 7900 RealTime PCR) with a 2% ramp rate. Fluorescent readings were recorded every 2 min. Following signal normalization, melting curves were generated from these data and analyzed in GraphPad using a Boltzmann sigmoidal analysis where analysis was restricted to boundaries that included the transition of interest. The T_m reported corresponds to the inflection point of the sigmoidal curve, which represents the temperature at which half of the population of the protein is unfolded. The T_m reported corresponds to the inflection point of the sigmoidal curve, which represents the temperature at which half of the population of the protein is unfolded. The resulting T_m was plotted as a scatter plot of each individual sample using GraphPad Prism. $NAA10_{1–160}$/$NAA15_{K450E}$ purified in the absence (-IP_6) and presence of 15 μM (+IP_6) was utilized in the assay with additional IP_6 to ensure a final concentration of 15 μM (+IP_6) after sample setup.

Pull-down assays

6xHis-tagged NatA (WT and L814P mutant) as well as MBP-tagged HYPK proteins were prepared as described above. Free MBP was prepared as described for MBP-HYPK above. The pull-down experiment represented in Figure 1S was conducted at 4°C where 2 μM prey (MBP-HYPK protein or free MBP) with 6 μM bait (6xHis-tagged hNatA WT or L814P mutant) were incubated together in sizing buffer 30 min. Proteins were then subjected to pull-down by incubation with amylose agarose resin (70 μl slurry, New England Biolabs, Ipswich, MA) for 30 min. Resin was washed with 80 CVs of sizing buffer before elution of bound proteins by boiling resin in SDS gel-loading buffer. Results of the pull-down assay were analyzed though visual inspection of the input and pull-down samples using 15% SDS-PAGE stained with Coomassie Brilliant Blue G-250.

Supplementary Material

Supplementary Material is available at *HMG* online.

Acknowledgements

The authors would like to thank the families who participated in this study. Ezzat El Ezzad, PhD. and Ms Mary Ellen Cafaro of the Graphic Resource and Media Service at New York State Institute for Basic Research in Developmental Disabilities provided photographic guidance in formatting family images for this article. The authors would like to thank the gnomAD and the groups that provided exome and genome variant data to this resource. A full list of contributing groups can be found at http://gnomad.broadinstitute.org/about.

Conflict of Interest statement. G.J.L. serves on advisory boards for Seven Bridges Genomics, Inc.; Phosphorus, Inc.; and Fabric Genomics, Inc.

Funding

Stanley Institute for Cognitive Genomics (G.J.L.); New York State Institute for Basic Research in Developmental Disabilities (G.J.L.); Health Innovation Challenge Fund (HICF-1009-003); Wellcome Trust Sanger Institute (WT098051); National Institutes of Health (R01 GM060293 and R35 GM118090 to R.M., T32 GM071339 to L.G.).

References

1. Van Damme, P., Evjenth, R., Foyn, H., Demeyer, K., De Bock, P.J., Lillehaug, J.R., Vandekerckhove, J., Arnesen, T. and Gevaert, K. (2011) Proteome-derived peptide libraries allow detailed analysis of the substrate specificities of N (alpha)-acetyltransferases and point to hNaa10p as the post-translational actin N (alpha)-acetyltransferase. *Mol. Cell. Proteomics*, **10**, M110.004580.
2. Dörfel, M.J. and Lyon, G.J. (2015) The biological functions of Naa10—from amino-terminal acetylation to human disease. *Gene*, **567**, 103–131.
3. Wu, Y. and Lyon, G.J. (2018) NAA10-related syndrome. *Exp. Mol. Med.*, **50**, 85.
4. Rope, A.F., Wang, K., Evjenth, R., Xing, J., Johnston, J.J., Swensen, J.J., Johnson, W.E., Moore, B., Huff, C.D., Bird, L.M. *et al.* (2011) Using VAAST to identify an X-linked disorder resulting in lethality in male infants due to N-terminal acetyltransferase deficiency. *Am. J. Hum. Genet.*, **89**, 28–43.
5. Saunier, C., Stove, S.I., Popp, B., Gerard, B., Blenski, M., AhMew, N., de Bie, C., Goldenberg, P., Isidor, B., Keren, B. *et al.* (2016) Expanding the phenotype associated with NAA10-related N-terminal acetylation deficiency. *Hum. Mutat.*, **37**, 755–764.
6. Popp, B., Stove, S.I., Endele, S., Myklebust, L.M., Hoyer, J., Sticht, H., Azzarello-Burri, S., Rauch, A., Arnesen, T. and Reis, A. (2015) De novo missense mutations in the NAA10 gene cause severe non-syndromic developmental delay in males and females. *Eur. J. Hum. Genet.*, **23**, 602–609.
7. Rauch, A., Wieczorek, D., Graf, E., Wieland, T., Endele, S., Schwarzmayr, T., Albrecht, B., Bartholdi, D., Beygo, J., Di Donato, N. *et al.* (2012) Range of genetic mutations associated

with severe non-syndromic sporadic intellectual disability: an exome sequencing study. *Lancet*, **380**, 1674–1682.
8. Casey, J.P., Støve, S.I., McGorrian, C., Galvin, J., Blenski, M., Dunne, A., Ennis, S., Brett, F., King, M.D., Arnesen, T. *et al.* (2015) NAA10 mutation causing a novel intellectual disability syndrome with Long QT due to N-terminal acetyltransferase impairment. *Sci. Rep.*, **5**, 16022.
9. Sidhu, M., Brady, L., Tarnopolsky, M. and Ronen, G.M. (2017) Clinical manifestations associated with the N-terminal-acetyltransferase NAA10 gene mutation in a girl: Ogden syndrome. *Pediatr. Neurol.*, **76**, 82–85.
10. Valentine, V., Sogawa, Y., Rajan, D. and Ortiz, D. (2018) A case of de novo NAA10 mutation presenting with eyelid myoclonias (AKA Jeavons syndrome). *Seizure*, **60**, 120–122.
11. Støve, S.I., Blenski, M., Stray-Pedersen, A., Wierenga, K.J., Jhangiani, S.N., Akdemir, Z.C., Crawford, D., McTiernan, N., Myklebust, L.M., Purcarin, G. *et al.* (2018) A novel NAA10 variant with impaired acetyltransferase activity causes developmental delay, intellectual disability, and hypertrophic cardiomyopathy. *Eur. J. Hum. Genet.*, **26**, 1294–1305.
12. McTiernan, N., Støve, S.I., Aukrust, I., Mårli, M.T., Myklebust, L.M., Houge, G. and Arnesen, T. (2018) NAA10 dysfunction with normal NatA-complex activity in a girl with non-syndromic ID and a de novo NAA10 p.(V111G) variant—a case report. *BMC Med. Genet.*, **19**, 47.
13. Esmailpour, T., Riazifar, H., Liu, L., Donkervoort, S., Huang, V.H., Madaan, S., Shoucri, B.M., Busch, A., Wu, J., Towbin, A. *et al.* (2014) A splice donor mutation in NAA10 results in the dysregulation of the retinoic acid signalling pathway and causes Lenz microphthalmia syndrome. *J. Med. Genet.*, **51**, 185–196.
14. Liszczak, G., Goldberg, J.M., Foyn, H., Petersson, E.J., Arnesen, T. and Marmorstein, R. (2013) Molecular basis for N-terminal acetylation by the heterodimeric NatA complex. *Nat. Struct. Mol. Biol.*, **20**, 1098–1105.
15. Gottlieb, L. and Marmorstein, R. (2018) Structure of human NatA and its regulation by the Huntingtin interacting protein HYPK. *Structure*, **26**, 925–935.e8.
16. Cheng, H., Dharmadhikari, A.V., Varland, S., Ma, N., Domingo, D., Kleyner, R., Rope, A.F., Yoon, M., Stray-Pedersen, A., Posey, J.E. *et al.* (2018) Truncating variants in NAA15 are associated with variable levels of intellectual disability, autism spectrum disorder, and congenital anomalies. *Am. J. Hum. Genet.*, **102**, 985–994.
17. Weyer, F.A., Gumiero, A., Lapouge, K., Bange, G., Kopp, J. and Sinning, I. (2017) Structural basis of HypK regulating N-terminal acetylation by the NatA complex. *Nat. Commun.*, **8**, 15726.
18. Arnesen, T., Starheim, K.K., Van Damme, P., Evjenth, R., Dinh, H., Betts, M.J., Ryningen, A., Vandekerckhove, J., Gevaert, K. and Anderson, D. (2010) The chaperone-like protein HYPK acts together with NatA in cotranslational N-terminal acetylation and prevention of Huntingtin aggregation. *Mol. Cell. Biol.*, **30**, 1898–1909.
19. Lyon, G.J. (2011) Personal account of the discovery of a new disease using next-generation sequencing. Interview by Natalie Harrison. *Pharmacogenomics*, **12**, 1519–1523.
20. Sharma, V.P., Fenwick, A.L., Brockop, M.S., McGowan, S.J., Goos, J.A.C., Hoogeboom, A.J.M., Brady, A.F., Jeelani, N.O., Lynch, S.A., Mulliken, J.B. *et al.* (2013) Mutations in TCF12, encoding a basic helix-loop-helix partner of TWIST1, are a frequent cause of coronal craniosynostosis. *Nat. Genet.*, **45**, 304–307.
21. Myklebust, L.M., Van Damme, P., Stove, S.I., Dörfel, M.J., Abboud, A., Kalvik, T.V., Grauffel, C., Jonckheere, V., Wu, Y., Swensen, J. *et al.* (2015) Biochemical and cellular analysis of Ogden syndrome reveals downstream Nt-acetylation defects. *Hum. Mol. Genet.*, **24**, 1956–1976.
22. Van Damme, P., Støve, S.I., Glomnes, N., Gevaert, K. and Arnesen, T. (2014) A *Saccharomyces cerevisiae* model reveals in vivo functional impairment of the Ogden syndrome N-terminal acetyltransferase NAA10 Ser37Pro mutant. *Mol. Cell. Proteomics*, **13**, 2031–2041.
23. Dorfel, M.J., Fang, H., Crain, J., Klingener, M., Weiser, J. and Lyon, G.J. (2017) Proteomic and genomic characterization of a yeast model for Ogden syndrome. *Yeast*, **34**, 19–37.
24. Szwergold, B.S., Graham, R.A. and Brown, T.R. (1987) Observation of inositol pentakis- and hexakis-phosphates in mammalian tissues by 31P NMR. *Biochem. Biophys. Res. Commun.*, **149**, 874–881.
25. Bittel, D.C., Theodoro, M.F., Kibiryeva, N., Fischer, W., Talebizadeh, Z. and Butler, M.G. (2008) Comparison of X-chromosome inactivation patterns in multiple tissues from human females. *J. Med. Genet.*, **45**, 309–313.
26. Richards, S., Aziz, N., Bale, S., Bick, D., Das, S., Gastier-Foster, J., Grody, W.W., Hegde, M., Lyon, E., Spector, E. *et al.* (2015) Standards and guidelines for the interpretation of sequence variants: a joint consensus recommendation of the American College of Medical Genetics and Genomics and the Association for Molecular Pathology. *Genet. Med.*, **17**, 405–424.
27. Kuo, H.P., Lee, D.F., Xia, W., Lai, C.C., Li, L.Y. and Hung, M.C. (2009) Phosphorylation of ARD1 by IKKbeta contributes to its destabilization and degradation. *Biochem. Biophys. Res. Commun.*, **389**, 156–161.
28. Kuo, H.P., Lee, D.F., Chen, C.T., Liu, M., Chou, C.K., Lee, H.J., Du, Y., Xie, X., Wei, Y., Xia, W. *et al.* (2010) ARD1 stabilization of TSC2 suppresses tumorigenesis through the mTOR signaling pathway. *Sci. Signal.*, **3**, ra9.
29. Kawaguchi, R., Yu, J., Honda, J., Hu, J., Whitelegge, J., Ping, P., Wiita, P., Bok, D. and Sun, H. (2007) A membrane receptor for retinol binding protein mediates cellular uptake of vitamin A. *Science*, **315**, 820–825.
30. Kawaguchi, R., Yu, J., Ter-Stepanian, M., Zhong, M., Cheng, G., Yuan, Q., Jin, M., Travis, G.H., Ong, D. and Sun, H. (2011) Receptor-mediated cellular uptake mechanism that couples to intracellular storage. *ACS Chem. Biol.*, **6**, 1041–1051.
31. Johnston, J.J., Williamson, K.A., Chou, C.M., Sapp, J.C., Ansari, M., Chapman, H.M., Cooper, D.N., Dabir, T., Dudley, J.N., Holt, R.J. *et al.* (2019) NAA10 polyadenylation signal variants cause syndromic microphthalmia. *J. Med. Genet.* **0**, 1–9.
32. Sobreira, N., Schiettecatte, F., Valle, D. and Hamosh, A. (2015) GeneMatcher: a matching tool for connecting investigators with an interest in the same gene. *Hum. Mutat.*, **36**, 928–930.